Biomass Conversion and Biorefinery (2023) 13:99–117
https://doi.org/10.1007/s13399-020-01160-8

ORIGINAL ARTICLE

# Extensive analyses of mass transfer, kinetics, and toxicity for hazardous acid yellow 17 dye removal using activated carbon prepared from waste biomass of *Solanum melongena*

Manish Chandra Kannaujiya [1,2] · Anuj Kumar Prajapati [2] · Tamal Mandal [1] · Ananta Kumar Das [3] · Monoj Kumar Mondal [2]

Received: 19 July 2020 / Revised: 17 November 2020 / Accepted: 18 November 2020 / Published online: 2 January 2021


## Abstract

The present study was focused on the synthesis of brinjal waste activated carbon (BWAC) from the dry woody part of brinjal plant by chemical activation method. The BWAC was used as adsorbent to remove acid yellow 17 (AY-17) from the synthetic solution. For BWAC synthesis, phosphoric acid was used as a chemical reagent for chemical activation at a ratio of 1:1, followed by pyrolysis of chemically treated biomass in $N_2$ atmosphere at high temperatures in a vertical reactor for improved chemical and surface properties of BWAC. The BWAC was characterized by several techniques such as BET surface area, pore distribution, SEM, FTIR, XRD, and point of zero charge ($pH_{PZC}$). Various affecting parameters such as equilibrium time, initial pH, BWAC dose, AY-17 concentrations, and temperature for dye removal by BWAC were also investigated in the batch experiment. The maximum of 99.58% removal of AY-17 dye by BWAC occurred at pH 3. More than 97% dye was removed by BWAC from aqueous solution for initial 15 mg/L AY-17 dye concentration with other conditions such as 2 g/L dose, 5.00 ± 0.2 pH, 80 min equilibrium time, and 25 °C temperature. Therefore, further experiments were carried out at pH 5. Equilibrium data were fitted with the isotherm models such as Langmuir, Freundlich, and Temkin, and according to the correlation coefficient ($R^2$), the Langmuir model was best fitted among them. The experimental kinetic data was well-validated with the pseudo-second-order kinetic model. The mass transfer studies of the dye onto BWAC were described by three models, such as Weber-Morris (intra-particle diffusion), Banghum's, and liquid film diffusion models, and the result reported that all steps were involved for the adsorption process. The order for the rate-determining step, according to $R^2$, was intra-particle diffusion > Bangham's model > liquid film diffusion model. Recovery and recycling of dye-treated BWAC with desorption efficiency of ~ 73% was possible by 1 M NaOH treatment after 5th cycles. The simulated dye solution after treatment by BWAC was used in seed germination for toxicity assessment.

**Keywords** Brinjal waste activated carbon (BWAC) · AY-17 · Isotherm model · Mass transfer · Toxicity assessment

## 1 Introduction

The excessive exploitation of global natural resources due to rapid industrialization leads to severe environmental problems including water and air pollution, biodiversity loss, and exhaustion of resources which have seriously affected the Earth's life support system [1]. Thus, in face of increased threats of water bodies from pollution, climate change, and ever-increasing population, the conservation of available freshwater resources and their maintenance has gained the urgency [2]. The leather industry is culpable for being a voracious of consumer of freshwater in large quantity for its various processing and non-processing activities and simultaneously releasing highly polluting wastewater. This would result in not only the water crisis for public but also pose threat to contaminate the ground water and running water with dyes, salts and other organic chemicals [3]. Leather dye effluent is one of the main polluting sources coming out from the tanning and dyeing processes [4]. Dyes are being designated as a stable compounds, so their presence in water are undesirable due

✉ Monoj Kumar Mondal
mkmondal13@yahoo.com

[1] Centre for Technological Excellence in Water Purification, Department of Chemical Engineering, National Institute of Technology Durgapur, Durgapur, India

[2] Department of Chemical Engineering and Technology, Indian Institute of Technology (Banaras Hindu University), Varanasi, Uttar Pradesh 221005, India

[3] Department of Environmental Science, Maulana Abul Kalam Azad University of Technology, Bidhannagar Kolkata, West Bengal, India

to difficult in degradation, lasting color, increase the chemical oxygen demand, and disturb the life activities of microorganism present in the aquatic environments [5]. A monoazo dye like acid yellow 17 (AY-17) which used in leather, paper and pulp, textile (dyeing silk, cotton, silk), and hot stamping foil is most problematic due to highly water soluble, as it tend to pass unaffected through conventional biological treatment system [6]. Beside, disperse dyestuffs have been found to have partition coefficient, resulting substantial potential for bioconcentration [7].

Strict environmental regulations have been established with the dyestuff for its discharge by many governmental agencies, which require associated industries to find economical, viable, and effective treatment technologies for effluents [4]. Most of the dyes used in leather industries for dying purposes are carcinogenic and mutagenic in nature. The presence of AY-17 dye in aqueous media creates severe environmental issues and also highly poisonous to human beings and animals. Sometimes, it undergoes chemical as well as biological changes, consumes soluble oxygen from the water bodies, and increases biological oxygen demand which leads to detrimental to the aquatic life [7]. Many health issues have been caused by adsorption of the azo dyes and their breakdown products (i.e., toxic amines) through gastrointestinal tract, skin, and lungs. It is harmful to respiratory system (i.e., dyspnea), skin (dermatitis), eyes (irritation to eyes), and cardiovascular and nervous system of human beings. Besides, it disturbs the blood formation by formation of hemoglobin adducts. Thus, it is very much essential to degrade and/or remove even a very small amount of the AY-17 dye from the effluents of the source industries [8].

During the past years, a number of treatment technologies, such as adsorption [9], coagulation-flocculation [10], advanced oxidation processes [11], membrane-based separation [12], ion-exchange resin, and biological treatment process [13] have been developed for the removal of dyes from the effluents. Most of the processes may be feasible for the treatment and/or removal of dyestuffs, but their initial capital investment and operation costs are huge that they cannot be applied widely at large scale amidst of emaciated profit margin by some industries, especially in developing countries [4]. Besides, several other disadvantages like large quantity of waste generation, incomplete treatment, and low selectivity are associated with some of the processes. Among various methods, adsorption-based treatment technology occupies a prominent place for the removal of dyestuffs due to cost-effective treatment process [14]. As eco-friendly and sustainable alternative to the traditional processes, adsorption has received an increasing attention in the removal of aqueous pollutants [15]. Adsorption of the toxic soluble dyes from the effluents through commercial activated carbon is highly efficient. However, high cost and 10–15% loss during regeneration has limited its use. Therefore, to minimize the treatment expenses incurred, low-cost, renewable, locally available, and effective alternative adsorbents are needed. Consequently, a number of renewable biomass and waste materials like *Typha angustata* L. [7], turmeric industrial waste [8], *Ipomoea carnia* stem waste [16], de-oiled soya, bottom ash [17], bagasse fly ash [18], activated sludge [19], coir pith [20], *Elaeagnus* stone [9], *Mangifera indica* sawdust [21], pecan nutshell [22], rambutan (*Nephelium lappaceum*) peel [23], etc. have been tried for the removal of dyes. Besides, magnetic adsorbent like activated carbon-$Fe_3O_4$ nanocomposite has also been applied for the sorption of AY-17 dye from aqueous phase [24]. However, agricultural waste-based activated carbons are widely used for removal of heavy metals and dyes containing wastewater because they have the high surface area, chemical stability, high adsorption capacities, and easy regeneration [25]. Similarly, in present investigation, dried brinjal (*Solanum melongena* L.) plant woody waste has been chosen as the precursor for the preparation of high surface area with great biosorptive efficiencies brinjal waste activated carbon (BWAC). It is commonly called aubergine in Europe and brinjal in India and belongs to Solanaceae family. To the best of our knowledge, there are no reports on the use of the woody waste of the *S. melongena* as adsorbent for the removal of AY-17 dye which is low cost, biodegradable, and poses no threat to the environment after disposal. According to the National Horticulture Board (NHB), such agricultural waste contains the huge amount of lignocellulosic substances having three main structural components: cellulose (approximately 65%), hemicelluloses (20–40%), and lignin (15–25%), besides extractives, lipids, sugars, proteins, water, and other compounds with different functional groups [26]. These ingredients are very useful in making a good adsorbent with some active sites like hydroxyl, carboxyl, methyl, amino, etc. which ensures high removal efficiency of aqueous pollutants [15].

Several chemical activating reagents such as NaOH, KOH, $ZnCl_2$, $H_3PO_4$, $K_2CO_3$, $Na_2CO_3$, etc. are used in literature. However, in present investigation, phosphoric acid is used as an activating agent because it is low corrosive and eco-friendly [27]. Thus, BWAC was synthesized, chemically activated by $H_3PO_4$, and subsequently characterized by BET, SEM, FTIR, and XRD analyses. In batch mode experiments, the synthesized BWAC was used to remove AY-17 dye from simulated solution with different operating parameters. The adsorption isotherms and kinetics models were fitted with experimental data to evaluate the model parameters. The mass transfer of dye from bulk of solution to BWAC was described by the Weber-Morris, layer film diffusion, and Bangham's models. Thermodynamics parameters such as $\Delta G°$, $\Delta H°$, and $\Delta S°$ were also estimated using the thermodynamic equation and van't Hoff plot. The reusability of BWAC adsorbent was also investigated with different eluents. The effect of seed germination was also studied with before and after adsorption of dye effluent.

## 2 Materials and methods

### 2.1 BWAC adsorbent preparation

The waste dried brinjal plant (BW) was collected from the local agricultural fields of Varanasi, Uttar Pradesh, India, and used as a raw precursor for the preparation of activated carbon from BW. The collected brinjal wastes were washed with tap water 2–3 times, and after then, it was washed with deionized water to remove unwanted impurities from the surface and then dried in the sun for 2–3 days. The dried wastes were cut into small pieces by disintegrator (Wiley mill model 2 (USA)) and then converted into powder with the help of a mixer grinder. The fine powder was sieved between 90 and 150 μm particle sizes by using mesh sieves. The particle size of the plant material influences many its properties and performances as an activated carbon such as stability in suspension, appearance, reactivity, viscosity, etc. The smaller particle sizes are more effective on the performances of adsorption as they yield larger external surface area resulting in availability of more active sites for adsorbing of solutes [28]. The chosen particle size range (90–150 μm) has also been selected by most of the authors in the literature [29, 30] for preparation of activated carbon for maximum adsorption of solute.

Ortho-phosphoric acid ($H_3PO_4$) (85% pure) was used as a chemical activating agent, and the brinjal waste powder was mixed with $H_3PO_4$ acid in 1:1 (*w*/*v*) ratio with the help of glass rod and kept for 12 h at room temperature following the method in the literature [30]. After that, chemically treated brinjal waste was washed with distilled water 3–4 times to remove excess acid. Then, chemically treated brinjal waste powder was dried in the hot air oven for 12 h at 105 °C. After drying, the chemically treated brinjal waste powder was pyrolyzed by using split tube furnace (Narang Scientific Works Pvt. Ltd., India) in the presence of $N_2$ gas in a tubular reactor at 700 °C for 90 min. The pyrolyzed material was cooled in room temperature in the flow of $N_2$ gas and then washed with diluted ammonia solution (A.G. Grade, RFCL Limited, New Delhi, India) and finally activated carbon washed with double-distilled water until the pH of filtrate solution has not reached up to 7 and then dried overnight at 90 °C. The dried samples were again sieved between 90 and 150 μm particle size, and BWAC was stored in an airtight container for future use.

### 2.2 Dye solution preparation and analysis

Leather dye AY-17 also known as acid yellow 2 GL was provided by a local tannery industry, Leder Chemical Pvt. Ltd., Kolkata, West Bengal, India. All the reagents used during the experiments were of analytical grade, and deionized water was used for the preparation of dye stock solution. The stock solution of 1000 mg/L AY-17 was prepared by dissolving 1000 mg of dye in 1 L distilled water, and it was diluted with distilled water for preparation of desired concentration. The stock solution of AY-17 was kept in the dark place to avoid the photo degradation due to the sunlight. The calibration curve for AY-17 was prepared by using a UV-Visible spectrophotometer by measuring the absorbance at the maximum wavelength ($\lambda_{max}$) of 402 nm.

### 2.3 Characterization

The important physicochemical properties like moisture content, volatile matter, ash content, and fixed carbon content were examined by carrying out proximate analysis. The different constituents of proximate analysis and method of analysis were followed according to the American Society for Testing and Materials such as moisture (ASTMD 5142), ash (ASTMD 3174), volatile content (ASTMD 872), and fixed carbon (ASTMD 3175). BET surface area and pore volume of BWAC were observed in $N_2$ atmosphere by adsorption/desorption technique at − 195 °C on an ASAP 2020 adsorption apparatus (Micromeritics). The point of zero charge of the BWAC was obtained by solid addition method [31]. The structural, functional groups and surface properties of BWAC were also characterized by FTIR, XRD, and SEM techniques. The FTIR analysis was obtained from an FTIR spectrometer (Thermo-Nicolson 5700, USA) using KBr as a reference chemical, the samples were passed into spectroscopic quality KBr and spectra were recorded in the range of 4000–400 $cm^{-1}$. The X-ray diffraction of BWAC before and after adsorption was recorded by Rigaku D/Max-B diffractometer with Cu Kα in the range of 10–80° (2θ). The surface physical morphologies of the BWAC after and before dye adsorption were identifying by using scanning electron microscope technique (ZEISS, EVO 18, Research, Germany).

### 2.4 Batch experimental studies

The BWAC was used for the adsorption of AY-17 by agitating known amount of BWAC with 100 mL of dye solution of desired concentration in Erlenmeyer flasks inside a water bath shaker at 120 rpm. Different operating parameters like concentration of AY-17 dye, contact time, initial solution pH, BWAC dosage, and reaction temperature were tested, and the remaining concentration of AY-17 was analyzed using Evolution™ 201 UV-Visible spectrophotometers (Thermo Fisher Scientific) at a wavelength of 402 nm. All kinetics experiments were done by using 0.2 g of BWAC in 100 mL simulated dye solution (15–60 mg/L of dye concentration) at 25 °C for 100-min treatment time. The flasks containing samples were agitated by using water bath shaker at 120 rpm. The flasks were taken at the regular time interval then centrifuged and measured the remaining concentration of dye. The effect of pH on adsorption of AY-17 was analyzed over the range of pH 1–11 by mixing of the desired amount of BWAC in

100 mL of 15 mg/L dye concentration. The BWAC dose effect on the adsorption process of AY-17 was carried out by mixing of the adsorbents ranging from 0.1 to 0.8 g in 100 mL of solution with varying concentrations from 15 to 60 mg/L at 25 °C. The thermodynamics of adsorption of AY-17 onto BWAC was study by mixing of 0.2 g BWAC in 100 mL solution having dye concentrations ranging from 15 to 300 mg/L. All experimental conditions for adsorption of AY-17 onto BWAC are shown in Table 1. The percentage removal and adsorption capacity of BWAC (mg/g) were calculated by using Eqs. (1) and (2), respectively.

$$\text{Percentage removal of AY-17 dye} = \left(\frac{C_{\text{i,AY}} - C_{\text{e,AY}}}{C_{\text{i,AY}}}\right) \times 100 \quad (1)$$

$$\text{Adsorption capacity (mg/g)} = \left(\frac{\left(C_{\text{i,AY}} - C_{\text{e,AY}}\right) \times \text{V}}{m}\right) \quad (2)$$

where $C_{\text{i,AY}}$ and $C_{\text{e,AY}}$ are the concentration of AY-17 (mg/L) at initially and equilibrium condition, respectively. $V$ (L) and $m$ (g) are the volume of solution taken in the experiment and the mass of BWAC, respectively.

### 2.5 $pH_{PZC}$ of BWAC

The point of zero charge of BWAC was determined by the pH titration [32] method. Fifty milliliters of 0.01 M $KNO_3$ was taken in eleven different flasks and the pH (2–12) was adjusted by the addition of 0.1 N HCl and NaOH solution. Fifty milligrams of BWAC was added in each flask, and the pH reading of suspension was taken after 48 h; the difference in initial pH and final pH was obtained. Finally, a graph (Fig. 1a) between initial pH verses ΔpH (initial pH − final pH) was drawn to obtain point of zero charge ($pH_{PZC}$) of BWAC.

### 2.6 Regeneration and reuse of BWAC

Initially, regeneration experiments were performed with four eluents such as NaOH, KOH, NaCl, and EtOH, for the determination of suitable eluent. The AY-17 dye-loaded BWAC obtained after treatment with 15 mg/L of dye at 25 °C for 120 min were used for the desorption experiment (Table 1). This dye-loaded BWAC was then brought into contact with 100 mL of eluents solutions of varying concentrations from 0.05 to 1 M for AY-17 dye desorption. The suspensions were agitated for 120 min at 25 °C with a shaking speed of 120 rpm, and final dye concentration after 1st desorption experiment was measured. After the selection of the suitable eluent, other cycles of adsorption-desorption experiments with that eluent were performed. After desorption, BWAC were washed with double-distilled water for two times and reused for the next cycle. Four sequential cycles of adsorption-desorption were carried out.

### 2.7 Effect of dye on seed germination

The seed germination of *Vigna radiata* (mung seeds) assessed the quality of treated effluent. Seed germination was done by untreated and treated solution [33]. Surface sterilization of healthy mung seeds of equal size was done with 70% ethyl alcohol followed by 0.1% (*w*/*v*) $HgCl_2$ for few minutes and washed with deionized water 4–5 times. Seed germination was done in moist filter paper in a petri dish with untreated effluent, treated effluent (dye concentration of 15, 30, 45, and 60 mg/L) and control (aqua guard water). Seed germination was done at room temperature, and its growth (root and shoot) was monitored and measured after 7 days of incubation.

## 3 Results and discussion

### 3.1 Characterization of BWAC

Characterization of BWAC was essential to know the physico-chemical and structural properties responsible for adsorption phenomena. The proximate analysis of raw BW was done and high carbon content was observed which signifies the applicability of BWAC to be used as adsorbent although significant amount of volatile matter was also detected. It was

**Table 1** Experimental condition for AY-17 dye adsorption onto BWAC adsorbent

| S. no. | Experimental parameters | Operating parameter range | | | | |
|---|---|---|---|---|---|---|
| | | Initial pH | BWAC dose (g/L) | Temperature (°C) | Initial AY-17 dye concentration(mg/L) | Contact time (min) |
| 1 | Equilibrium time | 5 | 2 | 25 | 15–60 | 10–100 |
| 2 | Initial pH | 3–11 | 2 | 25 | 15 | 80 |
| 3 | BWAC dose | 5 | 1–8 | 25 | 15–60 | 80 |
| 4 | Temperature | 5 | 2 | 25–45 | 15–300 | 80 |
| 5 | Desorption | – | 2 | 25 | 15 | 120 |

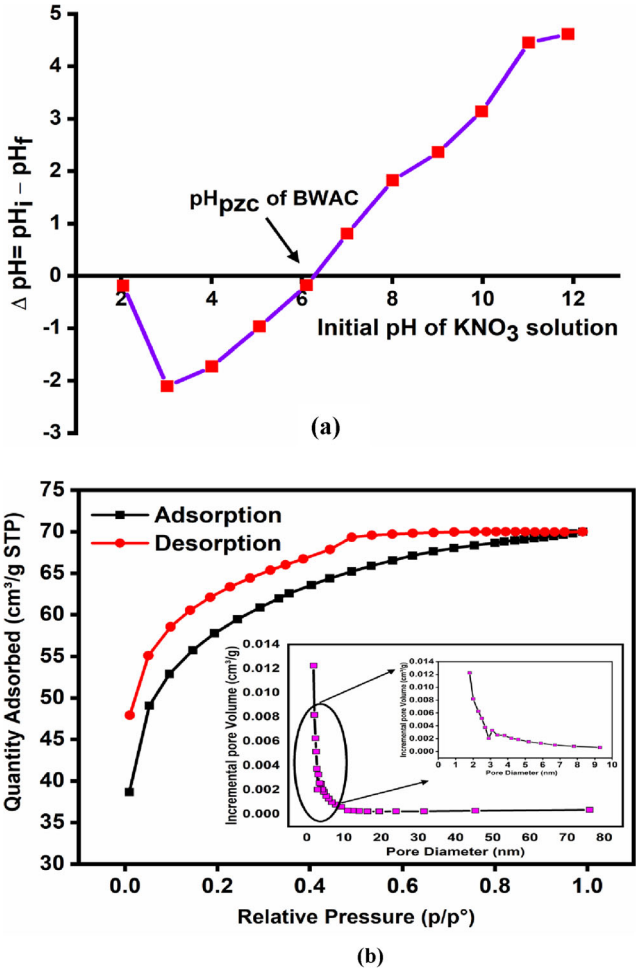


**Fig. 1** (**a**) Point of zero charge analysis of BWAC, **b** $N_2$ adsorption-desorption isotherm of BWAC (inserted pore size distribution of BWAC)

evident from the analysis that BW contained moisture (4.5%), volatile matter (11.8%), ash content (24.5%), and fixed carbon (59.2%). The low moisture and ash content with high content of fixed carbon were favorable properties of the biomass for the adsorbents [29]. The unstable organic substances at high temperature during carbonization and activation result into the breakdown of bonds and linkages of the molecules. Further, the volatile matters are released as gas and liquid products evaporates off turning a material with high carbon content and increased surface area as well as number of micro-pores within the surface [34].

The BET (Brunauer-Emmett-Teller) surface analyzer was performed to find the textural properties through pore volume as well as surface area of the adsorbents. The nitrogen adsorption-desorption isotherms of the BWAC was shown in Fig. 1b which confirmed that type I isotherm of the adsorbent. This indicates that the nitrogen molecules are absorbed mainly in the micro porous structure, but some part of nitrogen molecules are also absorbed in mesopores (2–50 nm) region of adsorbent [35]. According to pore size distribution as shown in Fig. 1b, the pore was concentrated in the micro porous range (< 2 nm) which signifies the adsorbent. The BET surface area (211.38 $m^2/g$), micropore volume (0.04828 $cm^3/g$), and average pore diameter (2.6 nm) of BWAC were observed which reflected the potential of BWAC as an effective adsorbent for AY-17 dye. This may be due to chemical activation of BW-derived biochar using phosphoric acid responsible for porous structure formation on the adsorbent surface [27]. The $pH_{PZC}$ of BWAC was found to be 6.31 which indicates that the BWAC exhibited positive charge at pH < 6.31, whereas negative charge surface at pH > 6.31.

The vibrational Fourier transform infrared (FTIR, Thermo-Nicolson 5700, spectrometer, USA) spectrum of adsorbent is shown in Fig. 2a. The surface functional groups of BWAC are more responsible for the adsorption of dye. The surface chemistry of BWAC is important aspect for adsorption that is well supported through the spectrum of FTIR in the range of 4000–500 $cm^{-1}$. The pellets were prepared by the mixing of BWAC with KBr in a proper ratio (1:99). The peaks between 2900 and

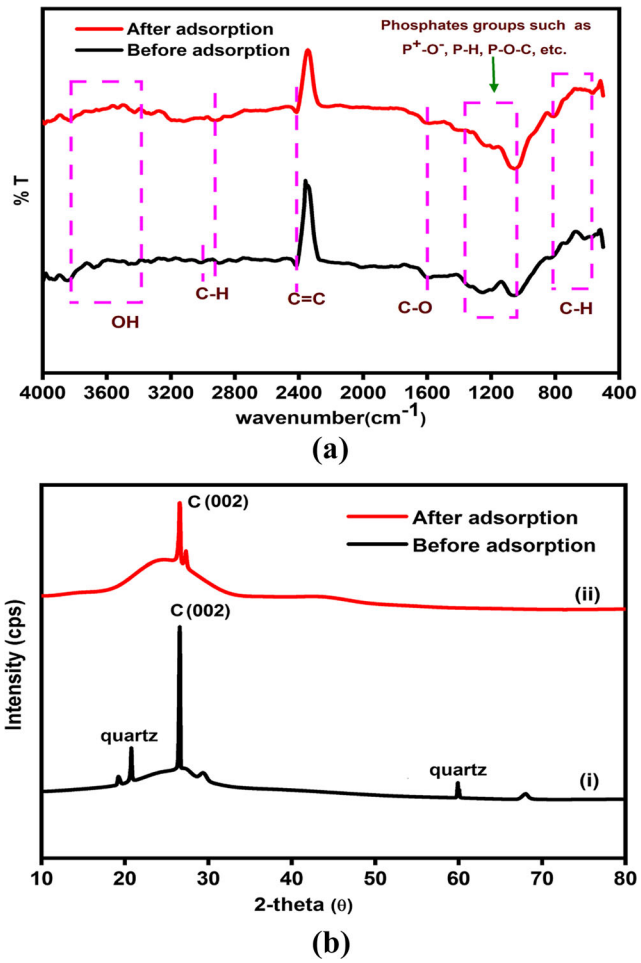


**Fig. 2** **a** FTIR analysis of BWAC (i) before and (ii) after AY-17 dye treatment. **b** XRD pattern of BWAC before and after AY-17 dye treatment

3900 $cm^{-1}$ of BWAC indicated the O–H stretching of the hydroxyl group from carboxyl, phenols, or alcohols as in cellulose, hemicelluloses, adsorbed water, and some lignin. These acidic and phenolic groups are responsible for AY-17 dye adsorption onto BWAC. The band at 2999.6 and 2890.2 $cm^{-1}$ is also assigned to the stretching of C-H representing such as alkanes groups, while peak at 2417 $cm^{-1}$ was due to the stretching vibration of C≡C bond in alkyne bonds [32]. A small intensity peak was appeared at 1620 to 1630 $cm^{-1}$ on BWAC due to the C-O stretching which is clearly indicative of a carboxylic acid compound [36]. The peak at 1181 $cm^{-1}$ is due C-N stretching vibration of amines group. The peak appeared between 900 and 1200 $cm^{-1}$ may be the presence of phosphate group species in the BWAC sample, such as stretching vibration of hydrogen-bonded P=OOH, $P^{+}$-$O^{-}$ in acid phosphate esters, P-H in phosphine group, and O-C stretching vibrations in P-O-C of aromatics [37]. The peaks located at approximately 814 and 621 $cm^{-1}$ are due to C–H bending and C–H out of plane vibrations, respectively. After the adsorption, the position of all peaks was shifted, and some peak disappeared, indicating that the adsorption process has occurred. The peaks were shifted or added to 1600 $cm^{-1}$ (C=C), 1250 $cm^{-1}$ (C-F), 1100 $cm^{-1}$ (P=O), and 785 $cm^{-1}$ (C-H) indicate adsorption of AY-17 dye.

The crystallite size and structure of BWAC were analyzed by XRD pattern as shown in Fig. 2b. A broad and sharp peak appeared at around 2θ = 22–28° (Fig. 2b (i)), showing that lattice miller indices is related to (002) graphitic carbon, indicating the amorphous nature of activated carbons [35]. The reason for the broad diffraction pattern is the presence of a small number of stacked graphite sheets. In addition, the BWAC sample showed some sharp peaks; the existence of these sharp peaks could be assigned to residual ash in carbon. The low-intensity peaks at approximately 2θ of 19°, 20°, and 60° also appeared in the XRD image (Fig. 2b (i)), which may be due to quartz lattice structure in BWAC due to high-temperature pyrolysis of BW. The metallic cristobalite is a high-temperature polymorph of silica which is present in the adsorbent. From the Scherrer equation, the average particle size of BWAC was 32.64 nm. The smaller size particles represent the greater surface area and may show better adsorption properties against the AY-17 dye. After adsorption, the intensity of the peak at approximately 2θ = 26° was decreased, and other peaks disappeared, indicating that adsorption of AY-17 dye occurred (Fig. 2b (ii)).

The surface morphological changes of BWAC were inspected by analysis of SEM images of before and after AY-17 dye treatment, are shown in Fig. 3 a and b, respectively. According to the SEM image, it was confirmed that the BWAC surface was heterogeneous and there were some micro size pores on the BWAC surface. That is a suitable condition for molecular diffusion along with providing greater surface area for dye adsorption. After adsorption, the surface of BWAC was smooth, and porosity decreased, which confirmed that the surface was occupied by AY-17.

### 3.2 Effects of contact time and initial dye concentration on the removal percentage

The effect of contact time is an important parameter to evaluate the kinetic rate constant and mass transfer coefficient, which are essential parameters to predict the order of reaction and mass transfer controlling step. It does not come into equilibrium condition until the adsorbate molecules have fully reached a saturation point on the adsorbent surface. Table 1 exhibits the contact time experimental condition for adsorption of AY-17 onto BWAC. The relation between removal percentage of AY-17 and contact time is shown in Fig. 4a**.** Results show that the removal efficiency of BWAC towards AY-17 dye was very fast at the initial stage and attained equilibrium at 80 min for all concentrations of AY-17 dye, and thereafter, the adsorption rate was more or less constant. The reason behind rapid adsorption was the availability of a large number of active sites on the adsorbent exteriors, and then it slowly decreased with increase of AY-17 dye attachment onto sorbent surface [38].

The initial AY-17 dye concentration also plays an important role in the adsorption process. Figure 4 a depicts the effect of different concentration of dye (15, 30, 45, and 60 mg/L) on their percentage removal by adsorbent. Results revealed that with increase in dye concentration, the gradual decrease in percentage removal of dye. Maximum removal of ~ 97% was observed at a dye concentration of 15 mg/L, then subsequently decreased to 95.8% (for 30 mg/L), 94.6% (45 mg/L), and 91.7% (45 mg/L) keeping the adsorbent dose fixed at 2 mg/L at 80 min of contact time. This can be attributed to the fact that at a fixed adsorbent dose and with an upsurge in initial dye concentration, all the available active sites were exhausted by dye molecules, which resulted in insufficient active groups on the adsorbent surface for further adsorption [39]. Thus, higher initial concentration of dye results in reduction in the initial rate of external diffusion as well as enhancement of intra-particle diffusion rate [29, 40].

### 3.3 Effects of initial pH on the removal percentage

The acidity/alkalinity of the solution shows a decisive role in AY-17 dye adsorption onto the BWAC. The aqueous chemistry of dye molecules in the aqueous phase and association/dissociation of functional groups present on the surface of the adsorbent is governed by the pH of the solution [29]. Thus, the performance of adsorption of the anionic dye (i.e., AY-17) onto BWAC is highly dependent on the initial pH of the solution, in which the adsorption occurred due to the strong interaction between the available electrophilic sites on the adsorbent surface and the anionic charge contained in the AY-17 dye molecules [41]. Furthermore, the surface chemistry of the adsorbent is highly dependent on the point of zero charge ($pH_{pzc}$) of the adsorbent, which is affected by changing the

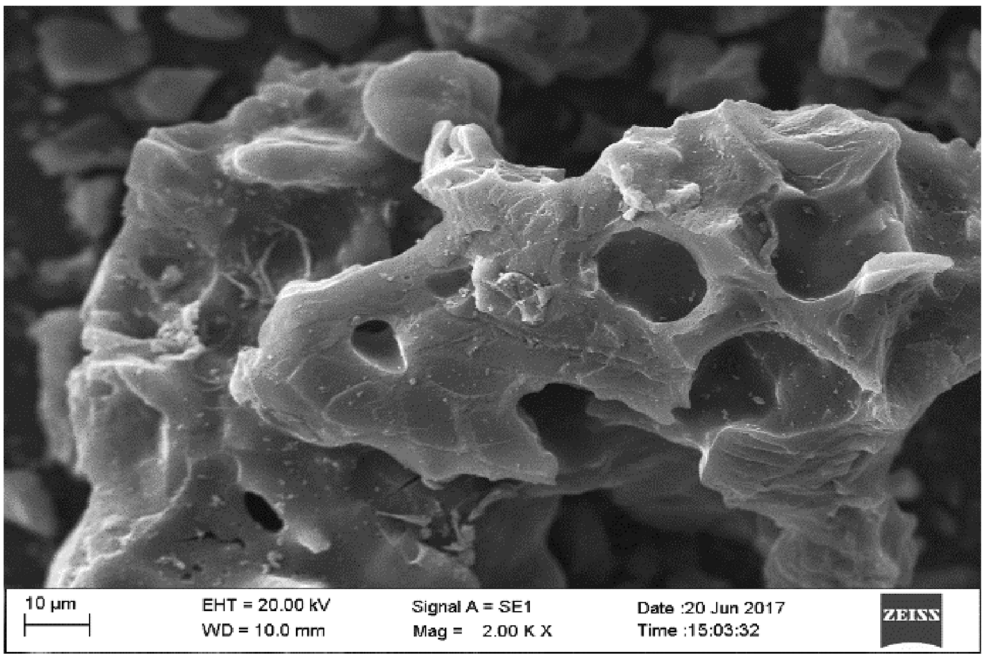


**(a)**

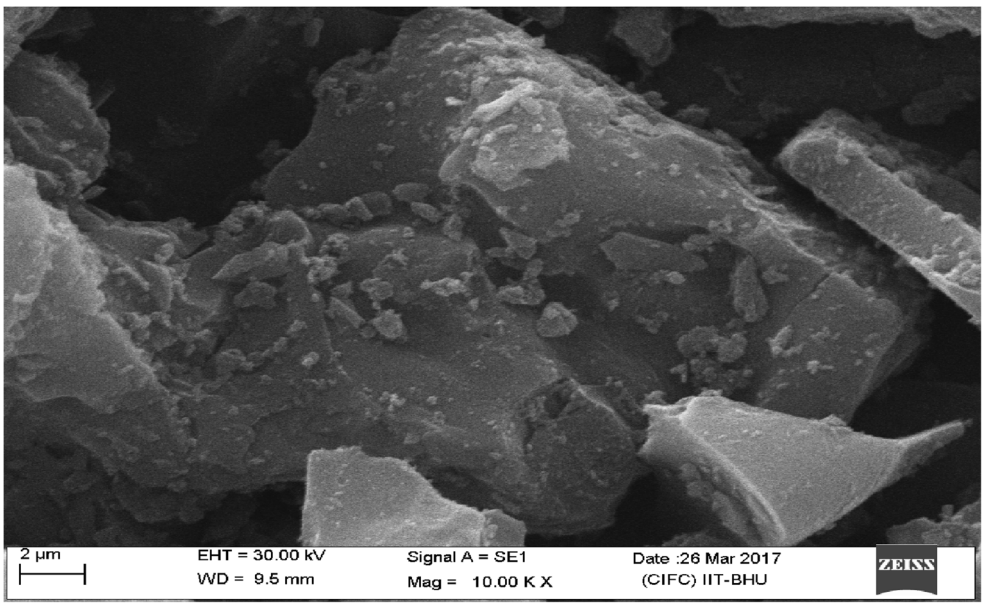


**(b)**

**Fig. 3** SEM images of BWAC (**a**) before AY-17 dye treatment **b** after AY-17 treatment

pH of the solution. The experimental conditions for the pH parameter are listed in Table 1, and Fig. 4b depicts the effect of the initial pH of solution on the adsorption of AY-17 dye onto BWAC. From Fig. 4b, it was noted that the adsorption of AY-17 dye decreased on increasing initial pH of the solution, and at pH 3, the maximum 99.58% dye was removed from the aqueous solution by BWAC. It was also notable that the removal percentage decreased by only 5.55% as compared to pH 3 when the pH of the solution was increased up to 6. Furthermore, at pH 11, the total reduction of removal percentage was more than 44% compared to pH 3. The maximum adsorption at pH 3 could have been due to the protonated surface formation, which was a more suitable condition for electrostatic attraction with the anionic dye. The functional groups (such as -OH,-CHO, -COOH, =CO, etc.) of adsorbent get protonated and take positive charge when the pH of the solution was below 6.31, which is the pHpzc of BWAC. Positively charged surface were attracted to anionic ion of

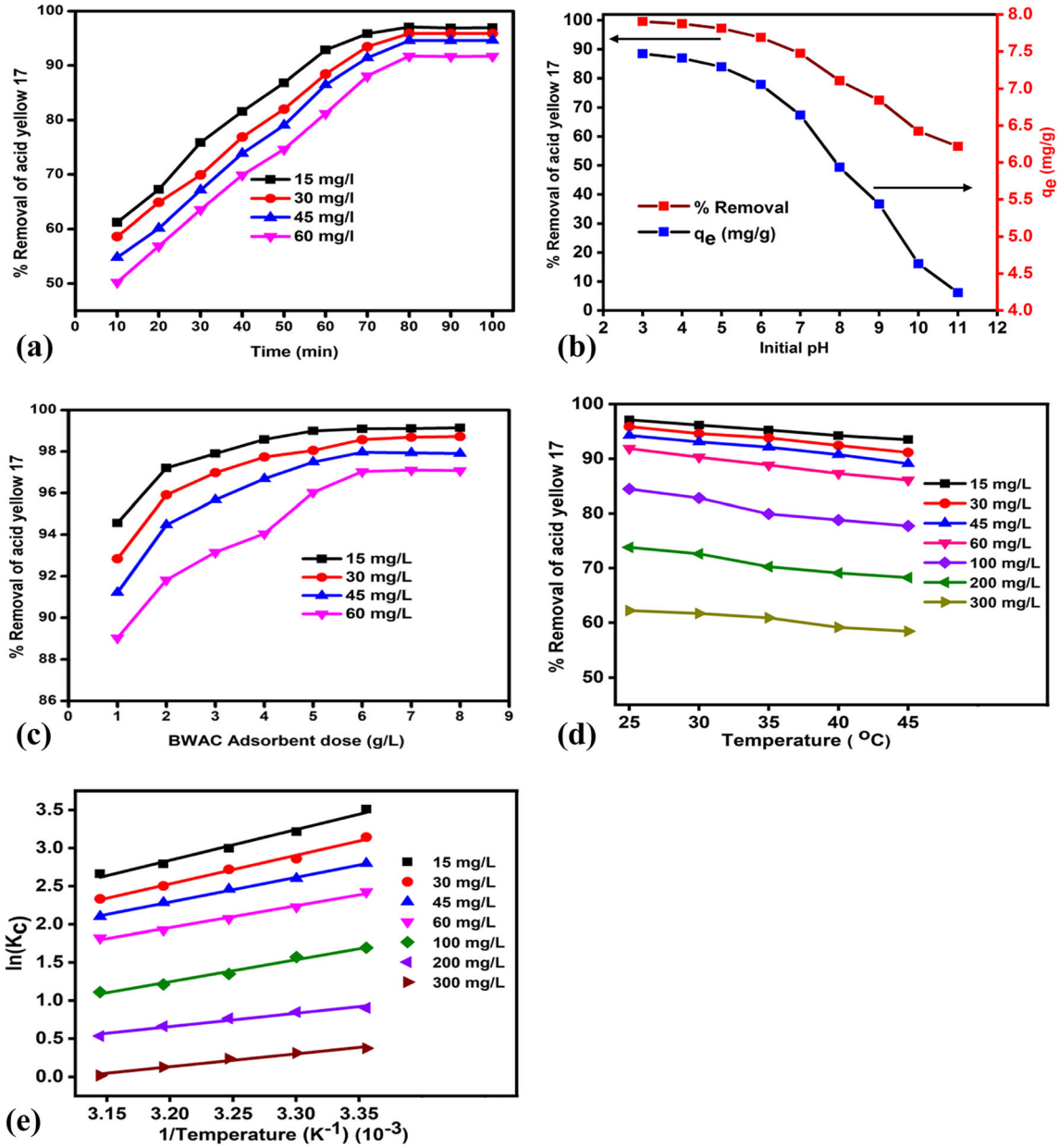


**Fig. 4** Effect of **a** contact time, **b** initial pH of solution, **c** BWAC adsorbent dose, and **d** reaction temperature on adsorption of AY-17 onto BWAC, and **e** van't Hoff plot for adsorption of AY-17 onto BWAC

$SO^{3-}$ formed in aqueous solutions of the dye. In contrast, the negative charge was dominated when the pH of the solution was higher than $pH_{pzc}$. Therefore, strong repulsion forces act between the negatively charged surface of BWAC and AY-17 dye. Moreover, electrostatic attraction, hydrogen bonding, and pore diffusion were also involved in the adsorption of AY-17 onto the BWAC adsorbent [42]. The possible reaction mechanism to illustrate this phenomenon is shown in Fig. 7b. Thus, the BWAC removes the AY-17 dye with remarkable efficiency of 99.58% at solution pH 3.0. The adsorption capacity of BWAC also showed a similar trend as the removal percentage (Fig. 4b), when the pH of the solution was raised from 3 to 11. This was due to decrease in the active sites responsible for capturing the dye molecules. Similar results were reported by Njoku et al., in which activated carbon was prepared from rambutan (*Nephelium lappaceum*) peel by microwave-induced KOH activation method and used for AY-17 dye adsorption. The results reported that the removal percentage was almost constant between pH 2 and 8 [23]. Over 97% removal by BWAC was shown to be at pH 5 in the present work, which was quite good, so for the stability and economic purpose of the adsorbent and use of treated wastewater in agricultural field as well, all other experiments were carried out at pH 5.

### 3.4 Effects of adsorbent dose and initial dye concentration on the removal percentage

The effect of initial AY-17 concentration on percentage removal by BWAC is an indispensable aspect of the applicability of the isotherm models. It also estimates the maximum adsorption capacity (mg/g) of BWAC. Table 1 shows the condition of parameters for adsorption of AY-17 onto BWAC. Figure 4 c illustrates the consequence of initial AY-17 concentration on percentage removal with different adsorbent doses. Removal of AY-17 dye was enhanced for all concentrations (15, 30, 45, and 60 mg/L) with increased adsorbent doses due to larger availability of active sites on the adsorbent surface for interaction with dye molecules [43]. Thus, as anticipated, an increase of sorbent dose from 1 to 6 g/L shows the positive correlation between sorbent doses with removal percentage of dye for all concentrations. However, further increase in the sorbent dose, there is no significant changes in the removal percentage of dye for all concentration and the relationship turned into stationary. This may be attributed to partial aggregation of biomass (adsorbent), which resulted in a reduction in effective surface area for sorption of dye molecules [4]. Maximum exclusion (99.2%) of dye was observed for 15 mg/L dye concentration at 6 g/L of adsorbent dose. However, removal percentage of dye marginally increased from 97.2 to 99.2% as the dose was increased from 2 to 6 g/L for 15 mg/L of dye concentration was observed. Thus, for economical and eco-friendly adsorption of AY-17 dye, adsorption dose of 2 g/L was critically appropriate to separate the dye from effluent successfully with minimum disposable of spent solid waste.

### 3.5 Effect of temperature

The effect of temperature on the removal percentage of AY-17 onto the BWAC is an essential parameter, which helps to investigate the effect of temperature on the removal percentage and to estimate the values of thermodynamic parameters such as Gibbs free energy ($\Delta G^0$), enthalpy change ($\Delta H^0$), and entropy change ($\Delta S^0$). Figure 4 d shows the effect of temperature on the removal percentage of AY-17 with varying the dye concentration from 15 to 300 mg/L, and all other experimental conditions were fixed, such as contact time 80 min, initial pH 5, and 2 g/L BWAC dose. The temperature profoundly influences the removal percentage of AY-17 dye from solution by BWAC. The results displayed in Fig. 4d confirmed that the removal percentage of AY-17 dye was decreased with the increased reaction temperature, and it also decreased with increasing initial dye concentrations. The removal percentage was decreased from ~ 97 to ~ 93%, ~ 95 to ~ 91%, ~ 94 to ~ 89%, ~ 91 to ~ 86%, ~ 84 to ~ 77%, ~ 73 to ~ 68%, and ~ 62 to ~ 58% for the 15, 30, 45, 60, 100, 200, and 300 mg/L dye concentrations, respectively, when the reaction temperature was increased from 25 to 45 °C, and confirmed that the adsorption phenomena was of exothermic nature [44]. The reason for this change may be increasing Brownian motion in solution and breakdown of hydrogen bonding at high temperatures that were formed between dye molecules with active functional groups of the BWAC [32]. Due to this, with increasing temperature of the solution, the AY-17 dye molecules leave from the solid phase (BWAC) and move towards the bulk liquid phase (AY-17 dye).

#### 3.5.1 Adsorption thermodynamic studies

To evaluate the feasibility of the adsorption process, it is essential to estimate thermodynamic parameters [45, 46]. Thermodynamic parameters studies are performed based on the effect of temperature on the adsorption of AY-17 by BWAC. The standard change in Gibbs free energy ($\Delta G^0$ (kJ/mol)) is an energy associated with a chemical reaction that is used to complete the reaction and estimated by Eq. 4. If the $\Delta G^0 < 0$, then the reaction is considered as spontaneous, and if $\Delta G^0 > 0$, then the chemical reaction is non-spontaneous. The enthalpy change $\Delta H^0$ (kJ/mol) is estimated the adsorption process is exothermic or endothermic. Similarly, entropy change ($\Delta S^0$ (J/mol K)) shows the intensity of randomness at the solid-liquid interface during the adsorption [32]. The following equations were used to calculate the standard change in free energy $\Delta G^0$ (kJ/mol), enthalpy change $\Delta H^0$ (kJ/mol) and entropy change $\Delta S^0$ (J/mol K) of the adsorption [42, 45]:

$$K_C = \frac{C_{ad}}{C_e} \tag{3}$$

$$\Delta G^O = -R*T*\ln(K_C) \tag{4}$$

$$\Delta G^O = \Delta H^0 - T\Delta S^0 \tag{5}$$

$$-R*T*\ln(K_C) = \Delta H^0 - T\Delta S^0 \tag{6}$$

where $R$, $K_c$, and $T$ are the universal gas constant (8.314 J/K mol), equilibrium constant, and temperature in Kelvin, respectively. The linear plots were drawn between ln $K_c$ vs. $1/T$ (van't Hoff plot) and used to calculate enthalpy and entropy from the slope and intercept, respectively (Fig. 1e) [32]. Table 2 shows the values of thermodynamic parameters such as $\Delta G^0$, $\Delta H^0$, $\Delta S^0$, and $R^2$. The negative values of $\Delta G^0$ confirmed that adsorption of AY-17 dye onto BWAC was a spontaneous process. Additionally, the values of $\Delta G^0$ were decreased with increasing temperatures, indicating that the adsorption process was unfavorable at the higher temperature. Therefore, adsorption process at higher temperature was not suitable for the adsorption of AY-17 by BWAC [47]. Similar results were also reported by Liu et al., where adsorption capacities of modified zeolites were favorable at low

**Table 2** Estimated values of $\Delta G^0$, $\Delta H^0$, $\Delta S^0$ and correlation coefficient for adsorption of AY-17 onto BWAC

| Parameter | | | | Temperature (K) | | | | |
|---|---|---|---|---|---|---|---|---|
| $C_0$(mg/L) | $\Delta H^0$(kJ/mol) | $\Delta S^0$(J/mol K) | $R^2$ | $\Delta G^0$ (kJ/mol) | | | | |
| | | | | 298 ± 1 | 303 ± 1 | 308 ± 1 | 313 ± 1 | 318 ± 1 |
| 15 | − 33.556 | − 83.772 | 0.980 | − 8.700 | − 8.096 | − 7.672 | − 7.258 | − 7.036 |
| 30 | − 31.260 | − 79.012 | 0.988 | − 7.788 | − 7.203 | − 6.960 | − 6.507 | − 6.165 |
| 45 | − 26.948 | − 67.196 | 0.996 | − 6.929 | − 6.547 | − 6.294 | − 5.939 | − 5.552 |
| 60 | − 23.779 | − 59.834 | 0.989 | − 6.004 | − 5.611 | − 5.309 | − 5.011 | − 4.814 |
| 100 | − 24.023 | − 66.512 | 0.986 | − 4.193 | − 3.955 | − 3.457 | − 3.155 | − 2.934 |
| 200 | − 14.559 | − 41.121 | 0.971 | − 2.239 | − 2.135 | − 1.960 | − 1.724 | − 1.409 |
| 300 | − 14.081 | − 43.971 | 0.979 | − 0.923 | − 0.780 | − 0.606 | − 0.327 | − 0.044 |

temperatures for anionic Congo red dye. The negative and decreasing values of $\Delta H^0$ (− 33.56 to − 14.08) confirmed that adsorption of AY-17 by BWAC was exothermic and adsorption process less feasible at higher temperatures. The negative $\Delta S^0$ (− 83.77 to − 43.97) values for different concentrations showed less randomness at the interface of liquid-solid phases during the adsorption process [4].

### 3.6 Adsorption kinetic models

The kinetic study gives more valuable information for the modeling and designing of adsorption processes. The time experimental data were analyzed with three traditional kinetic models such as pseudo-first-order, pseudo-second-order, and Elovich models to determine the adsorption behavior and kinetic parameters of AY-17 by BWAC [42, 48]. The linear form of the pseudo-first-order kinetic model can be expressed in Eq. (7):

$$\log(q_e - q_t) = \log(q_e) - \left(\frac{k_1}{2.303}\right) \times t \tag{7}$$

where $k_1$, $q_e$, and $q_t$ are rate constant of pseudo-first-order kinetic (1/min), equilibrium adsorption capacity of BWAC (mg/g), and adsorption capacity of BWAC at time "$t$" (mg/g). The value of $k_1$ and $q_e$ was calculated using a linear plot between log ($q_e$-$q_t$) vs. $t$, as shown in Fig. 5a. The pseudo-second-order kinetic model can be represented by the following Eq. (8):

$$\frac{t}{q_t} = \frac{1}{k_2 q_e^2} + \frac{t}{q_e} \tag{8}$$

where $k_2$ is rate constant of pseudo-second-order kinetic and its unit is g/mg min [49]. Figure 5 b shows the linear relationship between $t/q_t$ vs. $t$, which is used to estimate the values of $k_2$ and $q_e$ (theoretical).

The Elovich kinetic model can be expressed by Eq. (9):

$$q_t = \left(\frac{1}{\beta}\right) \ln \alpha\beta + \frac{1}{\beta} \ln t \tag{9}$$

where $\alpha$ and $\beta$ are initial AY-17 adsorption rate (mg/g min) and Elovich constant (g/mg), respectively, which depicts the surface coverage for chemisorption, and these can be calculated from the intercept and slope of the linear plot between $q_t$ vs. ln$t$, as shown in (Fig. 5c).

The kinetic studies of the adsorption process of AY-17 dye onto BWAC was investigated at 15–60 mg/L initial AY-17 concentrations by the pseudo-first-order model, pseudo-second-order model, and Elovich model equations, and the outcomes are illustrated in Fig. 5a–c and Table 3.

The correlation coefficients ($R^2$) and calculated adsorption capacity values ($q_{e,\mathrm{Cal}}$) were determined from the pseudo-first-order kinetic model, and Table 3 shows that the correlation values were significantly lower for all concentrations and calculated adsorption capacities are incomparable with experimental capacities values ($q_{e,\mathrm{Exp}}$), indicating that the adsorption process did not fit well with a pseudo-first-order kinetic model. From Table 3, the estimated values of $R^2$ were too high ≥ 0.99–0.984, and $q_{e,\mathrm{Exp}}$ values closed to $q_{e,\mathrm{Cal}}$ for the all concentrations of AY-17 dye when experimental data were linearly fitted with the pseudo-second-order kinetic model. Thus, adsorption of AY-17 dye onto BWAC followed the pseudo-second-order kinetic model; hence, adsorption phenomena occur through the chemisorption process, involving valence forces through the sharing of electrons between the adsorbent surface and adsorbate molecules [42].

The calculated values of $R^2$ for the Elovich kinetic model were low as compared to the pseudo-second-order kinetic model for all concentration cases and lies between 0.964 and 0.944 (Table 3). Hence, the sequence of the best linear fit, according to $R^2$, in general, was pseudo-second-order > Elovich model > pseudo-first-order.

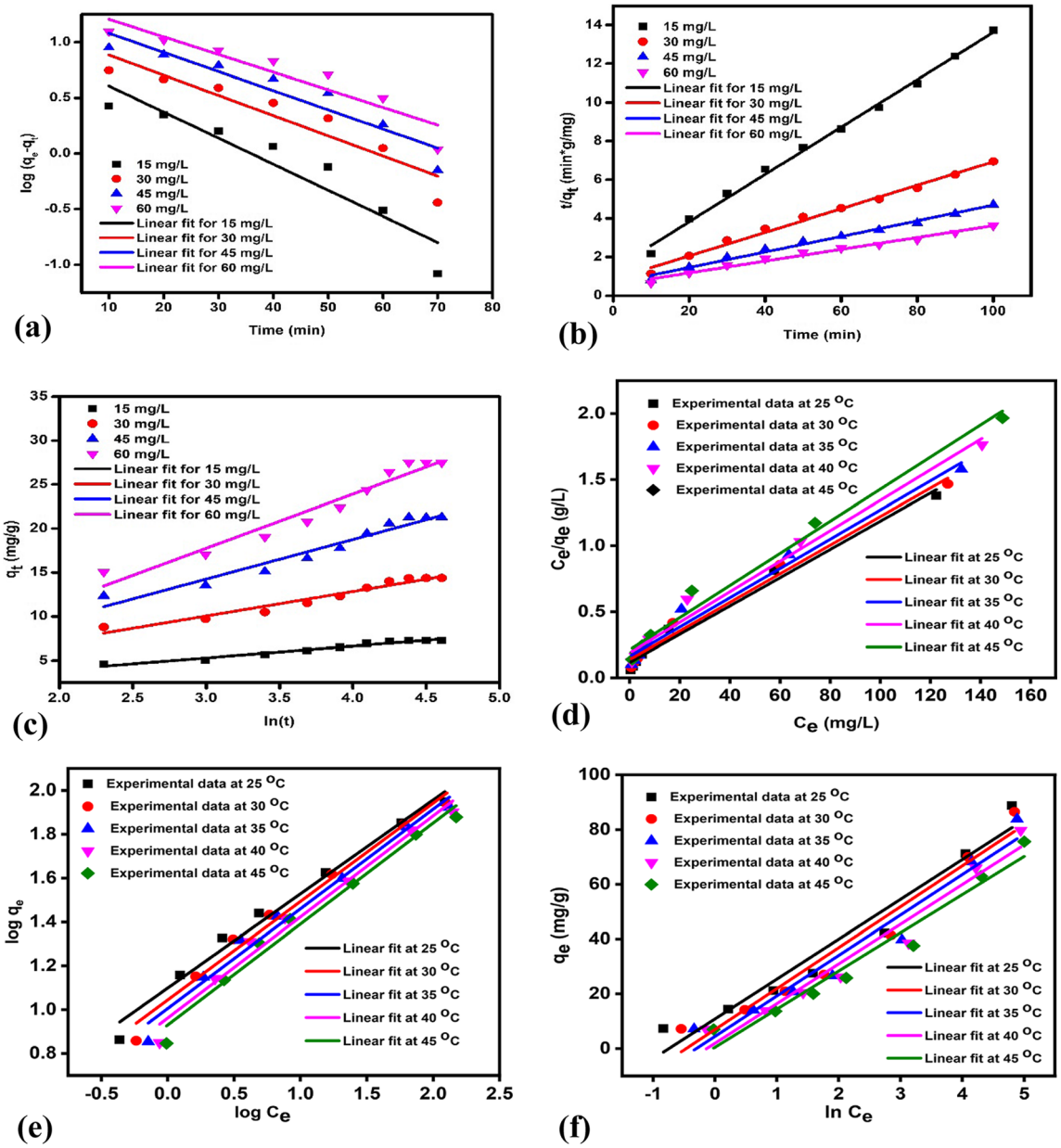


**Fig. 5** Linear fitted kinetic models: **a** pseudo-first-order, **b** pseudo-second-order, and **c** Elovich model. Linear fitted isotherm models: **d** Langmuir, **e** Freundlich, and **f** Temkin model

### 3.7 Isotherm models for AY-17 dye adsorption onto BWAC

Adsorption isotherms are essential and used extensively in deciding the maximum adsorption capacity of BWAC. It also helps to predict the adsorption mechanism and to design the adsorption system. Adsorption isotherm was an equilibrium condition when adsorbate molecules were adsorbed on the adsorbent surface with homogenous or heterogeneous or by both at constant temperature. In the present study, the experimental data were linearly fitted with three traditional isotherm models such as Langmuir [50], Freundlich [51], and Temkin isotherm model [52].

Langmuir model represents the equilibrium relationship between pollutant species concentration (adsorbate) with the number of active sites onto the adsorbent surface. The linear form Langmuir adsorption isotherm was expressed as:

$$\frac{Ce}{q_e} = \frac{1}{q_m K_L} + \frac{1}{q_m} Ce \tag{10}$$

where $q_e$, $C_e$, and $q_m$ are the experimental adsorption capacity of adsorbent (mg/g), equilibrium AY-17 dye concentration (mg/L), and theoretical maximum adsorption capacity (mg/g), respectively. $K_L$ is Langmuir constant (L/mg). The linear plot draw between $C_e/q_e$ and $C_e$ was used for the calculation of

**Table 3** Estimated values for adsorption kinetic model parameters for the adsorption of AY-17 dye onto BWAC

| Kinetic model | Experimental parameters | Acid yellow 17 concentration (mg/L) | | | |
|---|---|---|---|---|---|
| | | 15 | 30 | 45 | 60 |
| | $q_{e,\ exp}$ (mg/g) | 7.28 | 14.38 | 21.26 | 27.52 |
| First-order kinetic | $q_{e,\ cal}$ (mg/g) | 6.94 | 11.64 | 17.87 | 23.13 |
| | $K_1$ (L/mg) | 0.054 | 0.042 | 0.039 | 0.037 |
| | $R^2$ | 0.870 | 0.857 | 0.877 | 0.854 |
| Second-order kinetic | $q_{e,\ cal}$ (mg/g) | 8.159 | 16.444 | 24.851 | 32.669 |
| | $K_2$[(g/mg min) | 0.011 | 0.004 | 0.002 | 0.002 |
| | $R^2$ | 0.996 | 0.991 | 0.989 | 0.984 |
| Elovich kinetic model | $\beta$ (g/mg) | 0.747 | 0.385 | 0.222 | 0.162 |
| | $\alpha$ (mg/g min) | 3.512 | 5.0879 | 5.302 | 5.483 |
| | $R^2$ | 0.964 | 0.947 | 0.945 | 0.944 |

$q_m$ and $K_L$ (Fig. 5d). The isotherm was either favorable or unfavorable depending on estimating the separation factor $R_L$ [53], and it can be represented as:

$$R_L = \frac{1}{1 + K_L \times C_i} \tag{11}$$

The value of $R_L$ indicates linear/irreversible isotherm ($R_L = 0$), favorable isotherm ($0 < R_L < 1$), and unfavorable ($R_L > 1$).

Freundlich [51] model usually used to describe the adsorption on a heterogeneous surface or surface supporting site of varied affinities [53]. The linear form of Freundlich adsorption isotherm model is given as:

$$\log\ q_e = \log K_F + \frac{1}{n}\log C_e \tag{12}$$

where $K_F$ ((mg/g) (L/mg)$^{1/n}$) and $n$ are the Freundlich constants and their values are calculated from the linear plot of log $q_e$ vs. log $C_e$ (Fig. 5e) and shown in Table 3.

Temkin isotherm gives the information about the interaction between adsorbent molecules and adsorbate species [52], and it can be expressed by the following equation:

$$q_e = B\ln A + B\ln C_e \tag{13}$$

where $A$ and $B$ are the Temkin constant, and $B = RT/b_t$, $R$ (universal gas constant), $T$ (absolute temperature) in Kelvin, and $b_t$ is the heat of adsorption. The values of $A$ and $B$ were found by linear plot with $q_e$ vs. ln $C_e$ as depicted in (Fig. 5f).

The adsorption isotherm experimental data for adsorption of AY-17 by BWAC was linearly fitted with Langmuir, Freundlich, and Temkin models. The values of $R^2$ and other model constants are depicted in Table 4. The $R^2$ values at all temperatures were higher for Langmuir, followed by Freundlich and Temkin, as shown in Table 4. According to $R^2$ values, it can be concluded that the Langmuir model was the best linear fitted with experimental data as compared to Freundlich and Temkin model. The maximum adsorption capacity ($q_m$) was varied from 93.55 to 82.31 mg/g from 25 to

**Table 4** Adsorption Isotherm model parameters for adsorption of AY-17 onto BWAC

| Isotherm model | Experimental parameters | Temperature (°C) | | | | |
|---|---|---|---|---|---|---|
| | | 25 | 30 | 35 | 40 | 45 |
| Langmuir | $q_m$ (mg/g) | 93.545 | 92.507 | 90.416 | 86.655 | 82.305 |
| | $K_L$ (L/mg) | 0.092 | 0.078 | 0.068 | 0.061 | 0.057 |
| | $R^2$ | 0.987 | 0.990 | 0.988 | 0.986 | 0.983 |
| | $R_L$ | 0.421 | 0.461 | 0.495 | 0.522 | 0.539 |
| Freundlich | $n$ | 2.329 | 2.227 | 2.198 | 2.167 | 2.169 |
| | $K_f$[(mg/g)/(mg/L)$^{1/n}$] | 12.554 | 11.078 | 10.120 | 9.155 | 8.506 |
| | $R^2$ | 0.981 | 0.983 | 0.981 | 0.980 | 0.978 |
| Temkin | $A$ (L/mg) | 2.102 | 1.592 | 1.347 | 1.141 | 1.032 |
| | $B$ | 14.561 | 14.955 | 14.786 | 14.501 | 13.949 |
| | $R^2$ | 0.953 | 0.955 | 0.950 | 0.954 | 0.958 |

**Table 5** Comparison of maximum adsorption capacity ($q_{max}$) of different adsorbents for removal of dyes from liquid

| S. no. | Adsorbents | Dyes | Adsorption capacity (mg/g) | References |
|---|---|---|---|---|
| 1. | Silica nanofiber | Acid yellow 17 | 40.32 | [2] |
| 2. | Ionene chloride modified silica NF | Acid yellow 17 | 84.75 | [2] |
| 3. | Activated carbons from rambutan peel | Acid yellow 17 | 197.16 | [23] |
| 4. | Magnetic activated carbon-$Fe_3O_4$nanocomposites | Acid yellow 17 | 100 | [24] |
| 5. | Mesoporous carbon material ST-A | Acid yellow 17 | 35 | [54] |
| 6. | Activated carbon (CWZ-22) | Acid yellow 17 | 46 | [54] |
| 7. | Orange peel | Acid violet 17 | 19.88 | [55] |
| 8. | Soya bean waste | Acid blue 25 | 38.3 | [56] |
| 9. | Activated pericarp of pecan | Acid blue 25 | 28.75 | [57] |
| 10. | Activated carbon from industrial waste | Rhodamine-B | 16.12 | [58] |
| 11. | Brinjal waste activated carbon | Acid yellow 17 | *93.55* | Present study |

45 °C temperatures. $R_L$ values for the initial AY-17 concentration of 15 mg/L at constant BWAC dose were found in the range of 0.421 to 0.539 for temperature range from 25 to 45 °C, indicating a favorable condition for adsorption. Table 5 shows the comparative study of maximum adsorption capacity ($q_{max}$) of different adsorbents reported earlier with the data obtained in this work. The data showed that the BWAC prepared from Brinjal woody waste can be used as an effective adsorbent for the removal of AY-17 from its simulated solution.

### 3.8 Mass transfer analysis

The adsorption phenomenon mainly depends on the mass transfer operation, and by the use of extensive mass transfer models, the rate-determining step of any adsorption process can be estimated [42, 59, 60]. Mass of adsorbate molecules is transferred from the homogeneous/heterogeneous surface of the adsorbent to the pores of the adsorbent, characterized by mass transfer constant [61]. In the case of adsorption of AY-17 onto BWAC, intra-particle diffusion, pore and liquid film

**Table 6** Mass transfer analysis for adsorption of AY-17 onto BWAC

| Mass transfer model | | Concentration (mg/L) | | | | |
|---|---|---|---|---|---|---|
| | | | 15 mg/L | 30 mg/L | 45 mg/L | 60 mg/L |
| Weber andMorris model | First stage | $K_{id(1)}$ (mg/g $min^{1/2}$) | 0.468 | 0.727 | 1.185 | 1.715 |
| | | $C_1$ | 3.063 | 6.492 | 8.473 | 9.570 |
| | | $R^2_1$ | 0.984 | 0.999 | 0.989 | 0.997 |
| | Second stage | $K_{id(2)}$ (mg/g $min^{1/2}$) | 0.541 | 1.237 | 1.985 | 2.778 |
| | | $C_2$ | 2.7086 | 3.652 | 3.967 | 2.999 |
| | | $R^2_2$ | 0.995 | 0.998 | 0.996 | 0.996 |
| | Third stage | $K_{id(3)}$ (mg/g $min^{1/2}$) | 0.0105 | 0.021 | 0.010 | 0.007 |
| | | $C_3$ | 7.373 | 14.179 | 21.181 | 27.577 |
| | | $R^2_3$ | 0.929 | 0.938 | 0.915 | 0.912 |
| | Overall stage | $K_{id(ov)}$ (mg/g $min^{1/2}$) | 0.435 | 0.923 | 1.492 | 2.044 |
| | | $C_{ov}$ | 3.303 | 5.767 | 7.318 | 8.242 |
| | | $R^2_{ov}$ | 0.955 | 0.973 | 0.974 | 0.978 |
| Bangham's model | | $Ko$(mL/(g/L)) ($10^{-3}$) | 8.562 | 8.091 | 7.077 | 6.800 |
| | | $\alpha$ | 0.660 | 0.642 | 0.653 | 0.627 |
| | | $R^2$ | 0.934 | 0.908 | 0.914 | 0.921 |
| Liquid film diffusion model | | $K_{FD}$ | 0.0542 | 0.0418 | 0.0399 | 0.0365 |
| | | $C$ | − 0.041 | − 0.211 | − 0.169 | − 0.172 |
| | | $R^2$ | 0.891 | 0.881 | 0.896 | 0.877 |

diffusion can explain the transfer of AY-17 molecules, or sometimes it is dominated by all of them. In the present study, Weber and Morris, Bangham's, and liquid film diffusion models were used to analyze mass transfer mechanisms and rate-controlling step.

Weber and Morris model was also known as the intra-particle diffusion model and widely used for predicting the rate-controlling step in the adsorption process [62]. The equation of Weber and Morris model can be expressed as [42]:

$$q_t = K_{id} t^{0.5} + C \tag{14}$$

where $q_t$, $K_{id}$, $t$, and $C$ are the adsorption capacity (mg/g) at the time ($t$), intra-particle diffusion constant ((mg/g (min)$^{0.5}$), contact time (min), and boundary layer thickness (mg/g), respectively. The values of $K_{id}$ and boundary layer thickness were estimated by linear plotting of the graph between $q_t$ vs. $t^{0.5}$. This model suggested that if the plot between $q_t$ versus $t^{0.5}$ was linear and passed through the origin, then the rate-controlling step was intra-particle diffusion. If the plot was linear but did not pass through the origin, the adsorption process involved some other rate-controlling steps [63]. It is clear from Fig. 6a that the multi-linearity plot did not pass through the origin and were divided into three sections for all concentrations, which indicated that multi-steps were involved in controlling the mechanism [42]. This result confirmed that intra-particle diffusion was not only a rate-controlling step; some other controlling steps were also involved in the rate-controlling of AY-17 adsorption, such as boundary layer diffusion, pore diffusion, etc. [2, 7]. The first section in the Weber-Morris plot described the film diffusion. In which AY-17 dye molecules were transferred from the liquid phase to the outer surface of the BWAC via a hydrodynamic boundary layer. The second section involved the diffusion of AY-17 dye molecules from the surface of the BWAC into micro-sized pores, known as intra-particle diffusion. In the final section, AY-17 dye molecules reached an equilibrium state with BWAC. Table 6 shows the values of the overall and sectional intra-particle rate constant, boundary layer thickness, and $R^2$ for all concentration ranges. The boundary layer thickness (C) values increased with increasing concentration of AY-17 dye (Table 6), which confirmed that the

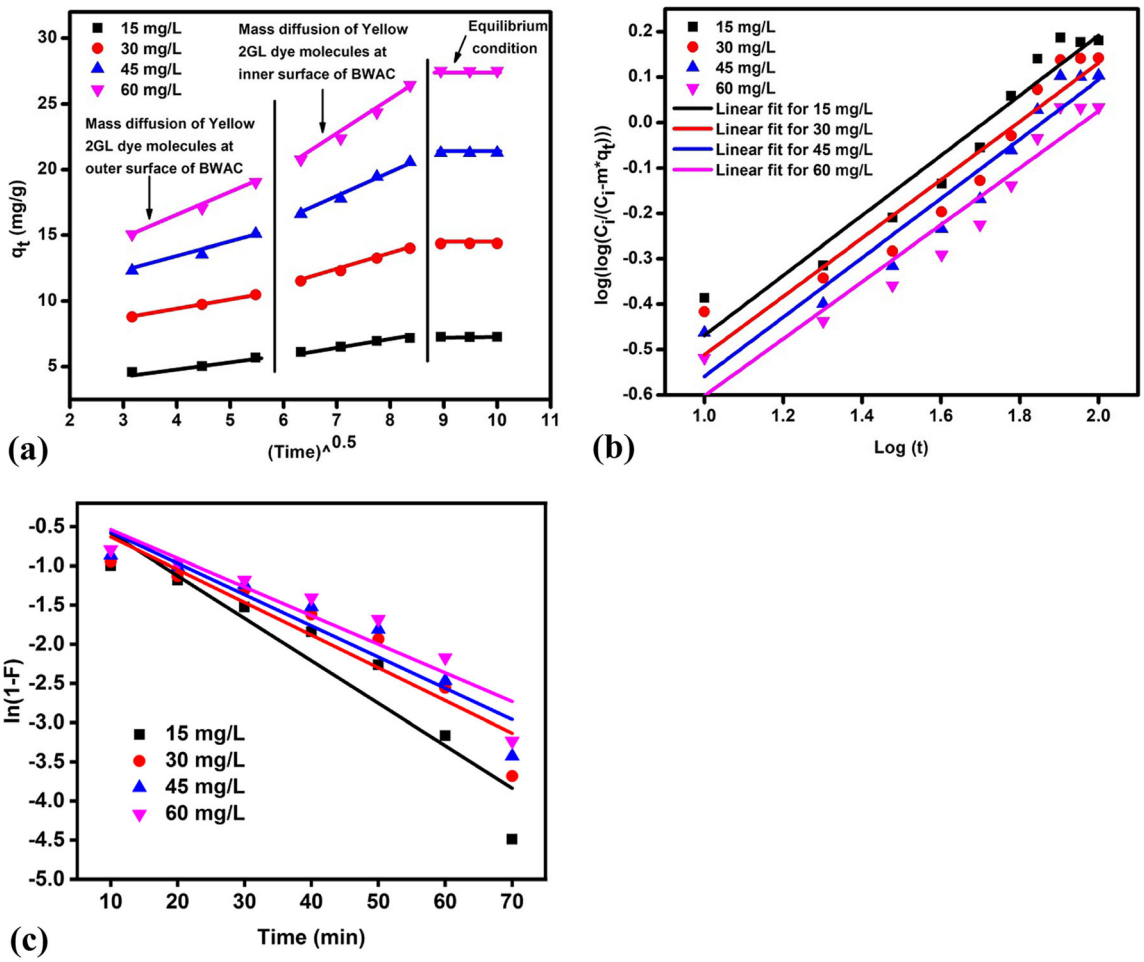


**Fig. 6** Mass transfer models: **a** Weber and Morris model, **b** Bangham's and Burt model, and **c** liquid film diffusion model for adsorption of AY-17 dye onto BWAC

boundary-layer diffusion mechanism was promoted at higher concentration of AY-17 dye.

If pore diffusion was an influential factor for adsorption of AY-17 onto BWAC, then Bangham and Burt model was used to check the rate-controlling step [64, 65]. Bangham's model is revealed by Eq. (15):

$$\text{loglog}\left(\frac{C_{i,\text{AY}}}{C_{i,\text{AY}}-q_t m_g}\right) = \log\left(\frac{k_B m_g}{2.303\, v_1}\right) + \alpha \log t \qquad (15)$$

where $C_{i,\text{AY}}$, $q_t$, $V_l$, and $m_z$ are the initial AY-17 concentration (mg/L), adsorption capacity at time "$t$" (mg/g), volume of solution (L), and mass in g/L of BWAC, respectively. Figure 6 b shows the linear plots of Bangham's model for the 15 to 60 mg/L concentrations of AY-17, and $\alpha$ and $k_B$ are the Bangham's constants, which were estimated from the linear plot between $\text{loglog}\left(\frac{C_i}{C_i - q_t m}\right)$ vs. log($t$). Table 6 shows the value of Bangham's constants and $R^2$. According to the $R^2$ and linear fitted plot, Bangham's model was not rate-determining step for the adsorption of AY-17 dye onto BWAC; it is also controlled by the boundary layer diffusion or both surface or pore diffusion.

The three-segmented curve of the Weber-Morris model gave the idea of the intentness of liquid film/layer diffusion for the adsorption of AY-17 dye onto BWAC in present work. Therefore, the film diffusion model was employed to equilibrium time data at four different concentrations (15 to 60 mg/L). Equation (16) represents the layer film diffusion model equation [42]:

$$\ln(1-f) = -K_{FD} \times t + \text{C} \qquad (16)$$

where $K_{FD}$ and $f = \frac{q_t}{q_e}$ are the film diffusion constant and fractional ratio of equilibrium adsorption capacities. The values of $K_{FD}$ and intercept were calculated by plots between ln(1-$f$) vs. $t$ and if the linear fitted plot passes through the origin, then liquid film diffusion was the rate-controlling step. Figure 6 c and Table 6 show the linear fitted plot and estimated values of $K_{FD}$ and intercept, respectively. The liquid film diffusion plot for AY-17 dye adsorption onto BWAC gave the linear plot for all concentrations with low $R^2$ and negative

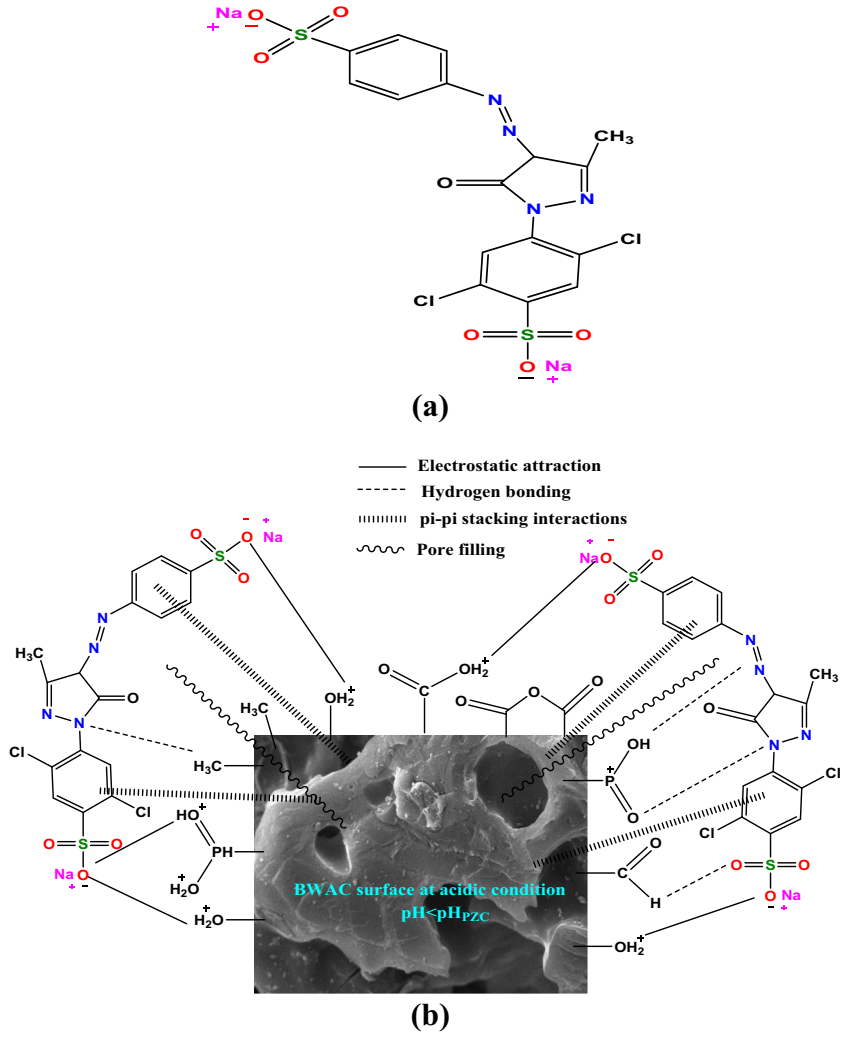


**Fig. 7** **a** Chemical structure of acid yellow-17 dye. **b** Possible reaction mechanism for the adsorption of AY-17 dye onto BWAC

intercept values. This result confirmed that liquid film diffusion was not a rate-determining step for the adsorption process. According to $R^2$ (Table 6) values from three mass transfer models, the rate-controlling sequence was intra-particles diffusion > Bangham's model > liquid film diffusion model. The original structure of AY-17 dye along with possible reaction mechanism for AY-17 dye adsorption onto BWAC is shown in Fig. 7.

### 3.9 Desorption and regeneration studies of adsorbent

Regeneration and reuse are necessary for the economical use of activated carbon as an adsorbent, which is an essential factor in determining adsorbent stability, economical cost of the waste treatment plant, and minimum waste discharge into the environment. The selection of suitable eluents is directly dependent upon the nature of the adsorption process; thus, NaOH, KOH, EtOH, and NaCl were used as eluents in desorption studies. In the present elution experiments (Fig. 8a), four eluents were used with varying concentrations from 0.05 to 1 M to determine which eluents would be suitable for the elution process of AY-17 dye-loaded BWAC. It was observed from the figure that the percentage desorption of AY-17 dye was 88.48, 75.88, 29.45, and 10.2% for 1 M concentration of NaOH, KOH, EtOH, and NaCl, respectively. The maximum desorption percentage AY-17 dye for all concentrations was higher in NaOH, followed by KOH, EtOH, and NaCl. In the first cycle of spent adsorbent, 88% of AY-17 dye was released from the dye-loaded BWAC. Batch studies of adsorption–desolation were repeated for four times with the same adsorbent, and the results are shown in Fig. 8b. The adsorption of AY-17 dye onto BWAC decreased by 3.81, 8.57, 16.11, and 24.38% in the second, third, fourth, and fifth cycles as compared to the initial adsorption rate, respectively. The adsorption of AY-17 dye in the 5th cycle was approximately 73%, which was 24% lower than the initial adsorption rate. This continuously decreasing adsorption rate may be due to excessive alkaline treatment, which results in damage to active groups or sites of BWAC and also reduced in surface area and pore volume of BWAC. Therefore, the AY-17 dye could be desorbed from AY-17 dye-loaded BWAC by NaOH, and 1 M NaOH solution concentration has excellent desorption performance than the other eluents. Thus, due to the superb adsorption-desorption performance, BWAC is a promising adsorbent for the AY-17 dye adsorption from aqueous solution.

### 3.10 Phytotoxicity assessment for environmental safety

Toxicity impact assessment for environmental safety was done with the treated simulated solution after AY-17 adsorption on plant growth and development. In present investigation, mung bean (*Vigna radiata*) seed germination bioassay was used as a biomarker due to quick growth, sensitive, and mostly grown pulses in the agricultural fields of the Indian subcontinent [66]. A toxicity study of treated and untreated samples of simulated dye solution was done by using equal-sized seeds of mung bean. The seeds were surface sterilized with 0.1% (*w*/*v*) $HgCl_2$ and 70% (*v*/v) EtOH followed by 3–4 times washing with deionized water. Seeds were germinated in petri-dish over filter paper in presence of Aquaguard water (control), simulated solution of four different concentrations (15 mg/L, 30 mg/L, 45 mg/L, and 60 mg/L) of AY-17 dye (untreated) and after the treatment of simulated solution of four different concentrations of dye (treated). The results were shown in Fig. 9 a and b as comparison of dye's effect on the growth of seed germination with concentrations for treated and untreated AY-17 dye solution. The untreated AY-17 dye solution had a toxic impact on the growth of seeds germination with a high concentration. The growth of seed was too slow for untreated dye solution as compared to BWAC treated dye effluent. Therefore, BWAC-treated dye effluent can be used in gardening and agriculture purposes after toxicity test.

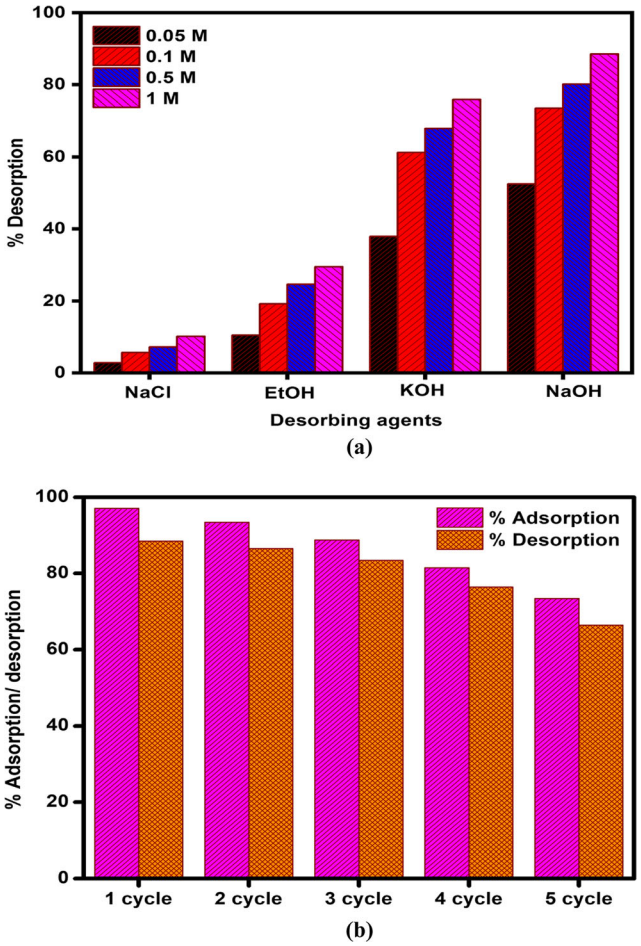


**Fig. 8** **a** % Desorption of AY-17 from BWAC with different desorbing reagents. **b** % Adsorption/desorption rate for AY-17 by BWAC up to 5th cycles

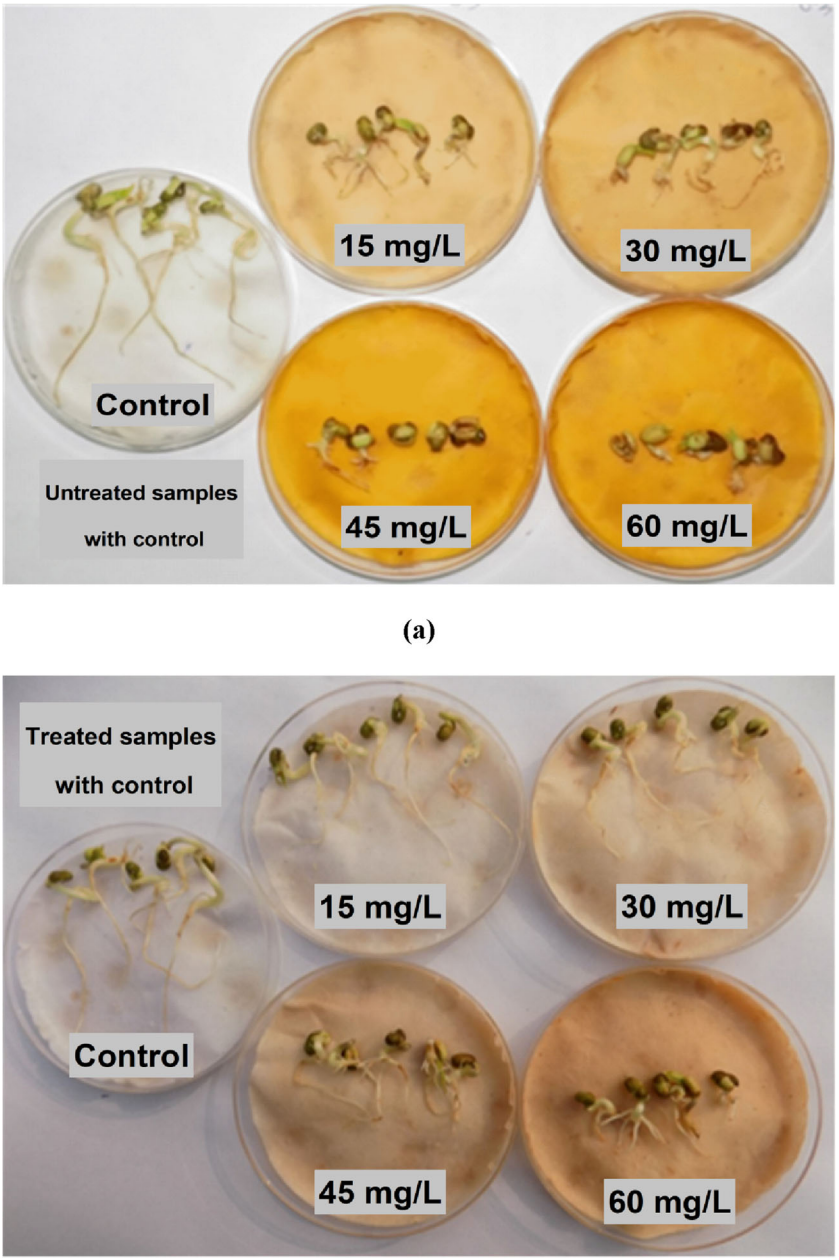


**Fig. 9** Effect of (**a**) before AY-17 dye treatment, (**b**) after treatment of AY-17 dye on seeds germination

## 4 Conclusions

Dried woody waste of *Solanum melongena* plant is available worldwide in large quantities, and that was used to synthesis of BWAC for removal of AY-17 from aqueous solution. The BWAC was characterized by SEM, XRD, FTIR, BET, and $pH_{PZC}$ analysis and results revealed that BWAC had heterogeneous and microsized pore surface, amorphous nature, high availability of functional groups (-OH, -COOH, =CO, P=OOH), and high surface area (211.38 $m^2/g$). The initial pH and concentration were profoundly impacted on percentage removal of AY-17, and removal of dye was suitable when the pH of the solution was lower than $pH_{PZC}$ of BWAC, and the maximum of 99.58% removal occurred at pH 3 for 15 mg/L dye concentration in 80 min contact time. The experimental data were best fitted with the Langmuir isotherm model as compared to Freundlich and Temkin models on the basis of $R^2$. Among various kinetic models, the pseudo-second-order kinetic model was superior to describe the adsorption kinetics of AY-17 dye onto BWAC**.** Mass transfer study confirmed that the transfer of AY-17 molecules from bulk phase to solid phase was not solely controlled by intra-particle diffusion; some other rate-controlling steps were also involved in reaction mechanisms such as liquid film diffusion and pore

diffusion. The sequence for the rate-determining step, according to $R^2$, was intra-particle diffusion > Bangham's model > liquid film diffusion model. Various desorbing agents were used in desorption study and 1 M NaOH showed the maximum desorption rate with ~ 88% for 1st cycle and decreased up to 73% in 5th cycle, which confirmed that BWAC exhibited good ability up to 5th cycles for removal of AY-17 dye. The treated effluent showed significant role for the germination of seeds which was able to support for the growth of mung bean (*Vigna radiata*) seeds.

**Acknowledgments** Manish Chandra Kannaujiya thanks the Chemical Engineering Department, NIT Durgapur, West Bengal, and Department of Chemical Engineering & Technology and CIF, Indian Institute of Technology (BHU), Varanasi, India, for providing necessary facilities and support at the time of work.

**Funding** This study is financially supported by the University Grants Commission, New Delhi, India (Grant No. F. 2-8/2005 (SA-1).

## References

1. Moktadir MA, Ahmadi HB, Sultana R, Zohra F-T, Liou JJH, Rezaei J (2019) Circular economy practices in the leather industry: a practical step towards sustainable development. J Clean Prod 251: 119737
2. Teli MD, Nadathur GT (2018) Adsorptive removal of acid yellow 17 (an anionic dye) from water by novel ionene chloride modified electrospun silica nanofibres. J Environ Chem Eng 6:7257–7272
3. Ali A, Shaikh IA, Abbasi NA, Firdous N, Ashraf MN (2020) Enhancing water efficiency and wastewater treatment using sustainable technologies: a laboratory and pilot study for adhesive and leather chemicals production. J Water Proces Eng 36:101308
4. Gao J, Zhang Q, Su K, Chen R, Peng Y (2010) Biosorption of acid yellow 17 from aqueous solution by non-living aerobic granular sludge. J Hazard Mater 174:215–225
5. Rosales E, Meijide J, Tavares T, Pazos M, Sanromán MA (2016) Grapefruit peelings as a promising adsorbent for the removal of leather dyes and hexavalent chromium. Process Saf Environ Prot 101:61–71
6. Aksu Z (2005) Application of adsorption for the removal of organic pollutants: a review. Process Biochem 40:997–1026
7. Ashraf MA, Hussain M, Mahmood K, Abdul Wajid A, Yusof M, Alias Y, Yusoff I (2013) Removal of acid yellow-17 dye from aqueous solution using eco-friendly adsorbent. Desal Water Treat 51:4530–4545
8. Karthikeyan KT, Jothivenkatachalam K (2014) Removal of acid yellow-17 dye from aqueous solution using turmeric industrial waste activated carbon. J Environ Nanotechnol 3(2):69–80
9. Gecel Ü, ÜnerO GG, Bayrak Y (2016) Adsorption of cationic dyes on activated carbon obtained from waste *Elaeagnus* stone. Adsorpt Sci Technol 34:512–525
10. Liang CZ, Sun SP, Li FY, Ong YK, Chung TS (2014) Treatment of highly concentrated wastewater containing multiple synthetic dyes by a combined process of coagulation/flocculation and nanofiltration. J Membr Sci 469:306–315
11. Chan SHS, Yeong-Wu T, Juan JC, Teh CY (2011) Recent developments of metal oxide semiconductors as photocatalysts in advanced oxidation processes (AOPs) for treatment of dye waste-water. J Chem Technol Biotechnol 86:1130–1158
12. Dutta M, Bhattacharjee S, De S (2020) Separation of reactive dyes from textile effluent by hydrolyzed polyacrylonitrile hollow fiber ultrafiltration quantifying the transport of multicomponent species through charged membrane pores. Sep Purif Technol 23:116063
13. Punzi M, Nilsson F, Anbalagan A, Svensson BM, Jonsson K, Mattiasson B, Jonstrup M (2015) Combined anaerobic-ozonation process for treatment of textile wastewater: removal of acute toxicity and mutagenicity. J Hazard Mater 292:52–60
14. Singh V, Srivastava VC (2020) Self-engineered iron oxide nanoparticle incorporated on mesoporous biochar derived from textile mill sludge for the removal of an emerging pharmaceutical pollutant. Environ Pollut 259:113822
15. Yuvaraja G, Krishnaiah N, Subbaiah MV, Krishnaiah A (2014) Adsorption of Pb(II) from aqueous solution by Solanum melongena leaf powder as a low-cost adsorbent prepared from agricultural waste. Colloids Surf B: Biointerfaces 114:75–81
16. Karthikeyan S, Bhuvaneswari G, Malathi S, Maheswari P, Sivakumar B (2007) Studies on removal of textile effluents using Ipomoea Carnea stem waste activated carbon. J Ind Council Chem 24:63
17. Gupta VK, Mittal A, Gajbe V (2005) Adsorption and desorption studies of a water soluble dye, Quinoline yellow, using waste materials. J Colloid Interface Sci 284:89–98
18. Gupta VK, Mohan D, Sharma S, Sharma M (2000) Removal of basic dyes (rhodamine B and methylene blue) from aqueous solutions using bagasse fly ash. Sep Sci Technol 35:2097–2113
19. Gulnaz O, Kaya A, Dincer S (2006) The reuse of dried activated sludge for adsorption of reactive dye. J Hazard Mater 134:190–196
20. Namasivayam C, Kavitha D (2002) Removal of Congo red from water by adsorption on to activated carbon prepared from coir pith, an agriculture solid waste. Dyes Pigments 54:47–58
21. Kapur M, Mondal MK (2013) Mass transfer and related phenomena for Cr (VI) adsorption from aqueous solutions onto *Mangifera indica* sawdust. Chem Eng J 218:138–146
22. Zazycki MA, Godinho M, Perondi D, Foletto EL, Collazzo GC, Dotto GL (2018) New biochar from pecan nutshells as an alternative adsorbent for removing reactive red 141 from aqueous solutions. J Clean Prod 171:57–65
23. Njoku VO, Foo KY, Asif M, Hameed BH (2014) Preparation of activated carbons from rambutan (*Nephelium lappaceum*) peel by microwave-induced KOH activation for acid yellow 17 dye adsorption. Chem Eng J 250:198–204
24. Ranjithkumar V, Hazeen AN, Thamilselvan M, Vairam S (2014) Magnetic activated carbon-Fe3O4 nanocomposites–synthesis and applications in the removal of acid yellow dye 17 from water. J Nanosci Nanotechnol 14:4949–4959
25. Rafatullah M, Sulaiman O, Hashim R, Ahmad A (2010) Adsorption of methylene blue on low-cost adsorbents: a review. J Hazard Mater 177:70–80
26. Nor NM, Chung LL, Teong LK, Mohamed AR (2013) Synthesis of activated carbon from lignocellulosic biomass and its applications in air pollution control—a review. J Environ Chem Eng 1:658–666
27. Chakraborty P, Show S, Rahman WU, Halder G (2019) Linearity and non-linearity analysis of isotherms and kinetics for ibuprofen removal using superheated steam and acid modified biochar. Process Saf Environ Prot 126:193–204
28. Raposo F, De La Rubia MA, Borja R (2009) Methylene blue number as useful indicator to evaluate the adsorptive capacity of granular activated carbon in batch mode: influence of adsorbate/adsorbent mass ratio and particle size. J Hazard Mater 165(1–3): 291–299
29. Srivastava S, Agrawal SB, Mondal MK (2015) Biosorption isotherms and kinetics on removal of Cr(VI) using native and chemically modified *Lagerstroemia speciosa* bark. Ecol Eng 85:56–66
30. Chakraborty P, Singh SD, Gorai I, Singh D, Rahman W-U, Halder G (2020) Explication of physically and chemically treated date

stone biochar for sorptive remotion of ibuprofen from aqueous solution. J Water Process Eng 33:101022
31. Narayan R, Meena RP, Patel AK, Prajapati AK, Srivastava S, Mondal MK (2015) Characterization and Application of biomass gasifier waste material for adsorptive removal of Cr (VI) from aqueous solution. Environ Prog Sustain Energy 35:1
32. Prajapati AK, Mondal MK (2019) Hazardous As(III) removal using nanoporous activated carbon of waste garlic stem as adsorbent: kinetic and mass transfer mechanisms. Korean J Chem Eng 36: 1900–1914
33. Kumar A, Priyadarshinee R, Singha S, Dasgupta D, Mandal T (2016) Rice husk ash based silica supported iron catalyst coupled with Fenton-like process for the abatement of rice mill wastewater. Clean Techn Environ Policy 18:2565–2577
34. Ahmad MA, Alrozi R (2010) Optimization of preparation conditions for mangosteen peel-based activated carbons for the removal of Remazol Brilliant Blue R using response surface methodology. Chem Eng J 165:883–890
35. Yakout SM, El-Deen GS (2016) Characterization of activated carbon prepared by phosphoric acid activation of olive stones. Arab J Chem 9:S1155–S1162
36. Lua AC, Yang T (2005) Characteristics of activated carbon prepared from pistachio-nut shell by zinc chloride activation under nitrogen and vacuum conditions. J Colloid Interf 290:505–513
37. Zhang X, Hao Y, Wang X, Chen Z (2017) Rapid removal of zinc (II) from aqueous solutions using a mesoporous activated carbon prepared from agricultural waste. Materials 10:1002
38. Kumar GV, Ramalingam P, Kim M, Yoo C, Kumar MD (2010) Removal of acid dye (violet 54) and adsorption kinetics model of using musa spp. waste: a low-cost natural sorbent material. Korean J Chem Eng 27:1469–1475
39. Mondal MK, Singh S, Umareddy M, Dasgupta B (2010) Removal of Orange G from aqueous solution by hematite: isotherm and mass transfer studies. Korean J Chem Eng 27:1811–1815
40. Mondal MK, Singh R, Kumar A, Prasad B (2011) Removal of acid red-94 from aqueous solution using sugar cane dust: an agro-industry waste. Korean J Chem Eng 28:1386–1392
41. Al-Degs YS, El-Barghouthi MI, El-Sheikh AH, Walker GM (2008) Effect of solution pH, ionic strength, and temperature on adsorption behavior of reactive dyes on activated carbon. Dyes Pigments 77: 16–23
42. Prajapati AK, Mondal MK (2020) Comprehensive kinetic and mass transfer modeling for methylene blue dye adsorption onto CuO nanoparticles loaded on nanoporous activated carbon prepared from waste coconut shell. J Mol Liq 307:112949
43. Pathania D, Sharma S, Singh P (2017) Removal of methylene blue by adsorption ontoactivated carbon developed from *Ficus carica* bast. Arab J Chem 10:S1445–S1451
44. Kapur M, Mondal MK (2014) Competitive sorption of cu (II) and Ni (II) ions from aqueous solutions: kinetics, thermodynamics and desorption studies. J Taiwan Inst Chem Eng 45:1803–1813
45. Suresh S, Srivastava VC, Mishra IM (2011) Isotherm, thermodynamics, desorption, and disposal study for the adsorption of catechol and resorcinol onto granular activated carbon. J Chem Eng Data 56:811–818
46. Wong S, Ghafar NA, Ngadi N, Razmi FA, Inuwa IM, Mat R, Amin NAS (2020) Effective removal of anionic textile dyes using adsorbent synthesized from coffee waste. Sci Rep 10:2928
47. Liu S, Ding Y, Li P, Diao K, Tan X, Lei F, Zhan Y, Li Q, Huang B, Huang Z (2014) Adsorption of the anionic dye Congo red from aqueous solution onto natural zeolites modified with N,N-dimethyl dehydroabietylamine oxide. Chem Eng J 248:135–144
48. Ho YS, Mckay G, Wase DAJ, Foster CF (2000) Study of the sorption of divalent metal ions on to peat. Adsorp Sci Technol 18:639–650
49. Nithya R, Thirunavukkarasu A, Sivashankar R, Rangabhashiyam S (2019) Fenalan Yellow G adsorption using surface-functionalized green nanoceria: an insight into mechanism and statistical modeling. Environ Res 181:108920
50. Langmuir I (1916) The constitution and fundamental properties of solids and liquids. J Am Chem Soc 38:2221–2295
51. Freundlich HMF (1906) Über die adsorption in lösungen. Z Phys Chem 57:385–470
52. Temkin MI, Pyzhev V (1940) Kinetics of ammonia synthesis on promoted iron catalysts. Acta Physiochim URSS 12:217–222
53. Zhang J, Li Y, Zhang C, Jing Y (2008) Adsorption of Melachite green from aqueous solution onto carbon prepared from *Arundo donax* root. J Hazard Mater 150:774–782
54. Jedynak K, Wideł D, Rędzia N (2019) Removal of rhodamine B (a basic dye) and acid yellow 17 (an acidic dye) from aqueous solutions by ordered mesoporous carbon and commercial activated carbon. Colloids Interfaces 3(1):30
55. Sivaraj R, Namasivayam C, Kadirvelu K (2001) Orange peel as an adsorbent in the removal of acid violet 17 (acid dye) from aqueous solutions. Waste Manag 21:105–110
56. Kooh MRR, Dahri MK, Lim LBL, Lim LH (2016) Batch adsorption studies on the removal of acid blue 25 from aqueous solution using *Azolla pinnata* and soya bean waste. Arab J Sci Eng 41:2453–2464
57. Hernández-montoya V, Mendoza-castillo DI, Bonilla-petriciolet A, Montes-Morán MA, Pérez-Cruz MA (2011) Role of the pericarp of *Carya illinoinensis* as adsorbent and as precursor of activated carbon for the removal of lead and acid blue 25 in aqueous solutions. J Anal Appl Pyrolysis 92:143–151
58. Kadirvelu K, Karthika C, Vennilamani N, Pattabhi S (2005) Activated carbon from industrial solid waste as an adsorbent for the removal of Rhodamine-B from aqueous solution: kinetic and equilibrium studies. Chemosphere 60:1009–1017
59. Rauthula MS, Srivastava VC (2011) Studies on adsorption/desorption of nitrobenzene and humic acid onto/from activated carbon. Chem Eng J 168:35–43
60. Thirunavukkarasu A, Nithya R (2020) Adsorption of acid orange 7 using green synthesized $CaO/CeO_2$ composite: an insight into kinetics, equilibrium, thermodynamics, mass transfer and statistical models. J Taiwan Inst Chem Eng 111:44–62
61. Banerjee S, Chattopadhyaya MC (2017) Adsorption characteristics for the removalof a toxic dye, tartrazine from aqueous solutions by a low cost agricultural by-product. Arab J Chem 10:S1629–S1638
62. Thirunavukkarasu A, Muthukumaran K, Nithya R (2018) Adsorption of acid yellow 36 onto green nanoceria and amine functionalized green nanoceria: comparative studies on kinetics, isotherm, thermodynamics, and diffusion analysis. J Taiwan Inst Chem Eng 93:211–225
63. Alhujaily A, Yu H, Zhang X, Ma F (2020) Adsorptive removal of anionic dyes from aqueous solutions using spent mushroom waste. Appl Water Sci 10:183
64. Bangham D, Burt F (1924) The behaviour of gases in contact with glass surfaces. Proc R Soc Lond A 105:481
65. Intriago LAZ, Mendoza MLG, Mosquera AC, Demera MHD, Duarte MMMB, Díaz JMR (2020) Kinetics, equilibrium, and thermodynamics of the blue 19 dye adsorption process using residual biomass attained from rice cultivation. Biomass Conv Bioref. https://doi.org/10.1007/s13399-020-00944-2
66. Kumar A, Priyadarshinee R, Singha S, Sengupta B, Roy A, Dalia Dasgupta D, Mandal T (2019) Biodegradation of alkali lignin by Bacillus flexus RMWW II: analyzing performance for abatement of rice mill wastewater. Water Sci Technol 80(9):1623–1632